Solar Energy 171 (2018) 658–666

Contents lists available at ScienceDirect

Solar Energy

journal homepage: www.elsevier.com/locate/solener

Solar synthesis of calcium aluminates

D. Fernández-González[a,*], J. Prazuch[b], I. Ruiz-Bustinza[c], C. González-Gasca[d], J. Piñuela-Noval[a], L.F. Verdeja[a]

[a] Department of Materials Science and Metallurgical Engineering, School of Mines, Energy and Materials, University of Oviedo, Oviedo, Asturias, Spain
[b] Department of Physical Chemistry and Modelling, Faculty of Materials Science and Ceramics, AGH University of Science and Technology, Krakow, Poland
[c] ETSI Minas y Energía, UPM, Madrid, Spain
[d] European University of Madrid-Laureate International Universities, Villaviciosa de Odón, Madrid, Spain

ARTICLE INFO

Keywords:
Concentrated solar energy
Calcium aluminate
Refractory cements
Environment
Refractory and ceramic materials
Solar energy

ABSTRACT

The production of high alumina refractory cements (> 75% Al_2O_3) is traditionally carried out in furnaces heated with both electric power (submerged arc furnaces) and fossil fuels (coke, natural gas). This heating system has several disadvantages: electricity price, contamination of the cement or greenhouse gases emissions. Solar energy, when properly concentrated, offers a great potential in high temperature applications, as those required in the manufacture of refractory and ceramic materials. In this paper we propose the synthesis of calcium aluminate compounds using concentrated solar energy. The results obtained prove the feasibility of the solar obtaining of the calcium aluminate compounds and could be useful for future development of this solar process in a larger scale.

1. Introduction

The production of cement is growing because of the increase in the world population but also due to the changes in construction methods in developing countries, and the improvement in infrastructures. In this way, the world production of Portland cement overcame the 4000 Mt in 2015 according to the USGS (United States Geological Survey). The production of cement has several problems: the first problem is that the production of cement is energy intensive (fuel and electricity consumption represent approximately a 40% of the total production costs (González and Flamant, 2014)); and the second problem is that the cement industry is environmentally non-friendly, being responsible for 5% of global anthropogenic CO_2, of which 50% is derived from the chemical process and 40% from burning fuel (Meier et al., 2005a).

Solar energy, when properly concentrated offers a lot of possible applications in different fields of materials science and metallurgy (Fernández-González et al., 2018). In this way, for instance, concentrated solar energy has been applied in the recovery of valuable components from the ironmaking and steelmaking industry (Ruiz-Bustinza et al., 2013; Mochón et al., 2014), in the production of silicon (Murray et al., 2006), in the carbothermal reduction of ZnO to be used in water splitting to produce H_2 (Osinga et al., 2004), in the obtaining of aluminium foams (García-Cambronero et al., 2008; García-Cambronero et al., 2010), in the sintering of high speed steels (Herranz et al., 2013; Herranz et al., 2014) or in surface treatment of steels (Llorente and Vázquez, 2009). In the field of non-metallic materials, concentrated solar energy has been applied since at least four centuries. In the 17th, Ehrenfried Walter Von Tschirnaus designed, constructed, and worked with lenses and mirrors with the purpose of concentrating solar energy, and, in this way, melting iron and obtaining ceramics (porcelain) (Gosh, 1991; Newcomb, 2009; McDonald and Hunt, 1982). Felix Trombe demonstrated the possible application of concentrated solar energy in the melting of high refractory ceramics (alumina, chromium oxide, zirconia, hafnia and thoria) after the Second World War (Flamant and Balat-Pichelin, 2010). More recent studies have widened the number of applications of concentrated solar energy in non-metallic materials. The manufacture of silicon carbide using concentrated solar energy was researched by several groups due to the large number of applications of this material (composite materials, combustible cells, electronics, etc.) (Cruz-Fernandes et al., 1998; Gulamova et al., 2009; Ceballos-Mendivil et al., 2015). Silicon nitride (Si_3N_4) with excellent properties (high fractures toughness, high flexural strength, and creep resistance even at high temperatures (Cardarelli, 2008)) was also synthesized in solar furnace (Zhilinska et al., 2003), the same as other materials with high wear resistance such as titanium carbide (Cruz-Fernandes et al., 1999; Cruz-Fernandes et al., 2002) and tungsten carbide (Guerra-Rosa et al., 2002). Other ceramic materials treated under concentrated solar energy were: alumina (Cruz-

* Corresponding author.
E-mail address: fernandezgdaniel@uniovi.es (D. Fernández-González).

https://doi.org/10.1016/j.solener.2018.07.012
Received 10 January 2018; Received in revised form 3 July 2018; Accepted 6 July 2018
Available online 12 July 2018
0038-092X/

Fernandes et al., 2000; Román et al., 2008) and cordierite (Costa-Oliveira et al., 2009).

The production of refractory and ceramic materials requires high temperatures (Verdeja et al., 2008; Verdeja et al., 2014; Pero-Sanz et al., 2017). Conventional technologies used in reaching such high temperatures require the utilization of electricity and/or the combustion of fossil fuels (Verdeja et al., 2008; Verdeja et al., 2014), causing both economic and environmental problems. Economically, the problems are mainly associated to the price of either the electricity or the fossil fuels, but also to the costs of releasing CO_2 (taxes associated to CO_2 emissions). Environmentally, the problems are linked to the emissions of CO_2 associated to the combustion of fuels used to reach the high temperatures (in the case of electric furnaces, the emissions associated to the production of electricity should be considered), but also other emissions such as SO_X and NO_X.

Calcium aluminate cements are the most important kind of non-Portland cements due to their properties (rapid hardening, resistance to high temperatures, resistance to temperature changes, resistance to chemical attack and resistance to impact and abrasion) (Scrivener, 2003). However, calcium aluminate cements are expensive and are used only in special applications. There are different types of calcium aluminate cements depending on the amount of the three constituents of the ternary diagram (CaO-SiO_2-Al_2O_3, see in Fig. 1 where calcium aluminate cements are in this ternary diagram), and according to Kurdowski, 2014 (page 604) these types of calcium aluminate cements are:

- Type 1: 37–40% Al_2O_3; 11–17% Fe_2O_3; 3–8% SiO_2; 36–40% CaO.
- Type 2: 48–51% Al_2O_3; 1–1.5% Fe_2O_3; 5–8% SiO_2; 39–40% CaO.
- Type 3: 51–60% Al_2O_3; 1–2.5% Fe_2O_3; 3–6% SiO_2; 30–40% CaO.
- Type 4: 78–80% Al_2O_3; 0–0.5% Fe_2O_3; 0–0.5% SiO_2; 17–27% CaO.

For instance, Almatis commercializes calcium aluminate cements with two qualities: 70% Al_2O_3 (25–30% CaO) and 80% Al_2O_3 (17–19% CaO), while the maximum levels for impurities is in both qualities of 0.3% Na_2O, 0.3% SiO_2, 0.2% Fe_2O_3 and 0.4% MgO. It is possible to stablish two groups of calcium aluminate cements: normal product, dark grey or black in color, used in a broad temperature range; white varieties, characterized by the high alumina contents, used for refractory purposes (Bensted, 2008). The manufacture of normal product quality is carried out by fusing a mixture of calcium carbonate (limestone) and ferruginous bauxite in reverberatory furnaces at 1500–1600 °C (Bensted, 2008). The heating of these furnaces is performed with pulverized coal, oil, natural gas, or a mixture of these fuels (Bensted, 2008). The production of white quality cement is carried out in rotary kilns by sintering or in electric arc furnaces also at high temperatures (Scrivener, 2003; Bensted, 2008). The main requirement is the purity of the raw materials (limestone and bauxite), which are expensive (Scrivener, 2003), and the heating should avoid the contamination of the cement by using specific combustibles with low level of impurities (Bensted, 2008). High alumina calcium aluminate refractory cements are for those reasons expensive materials.

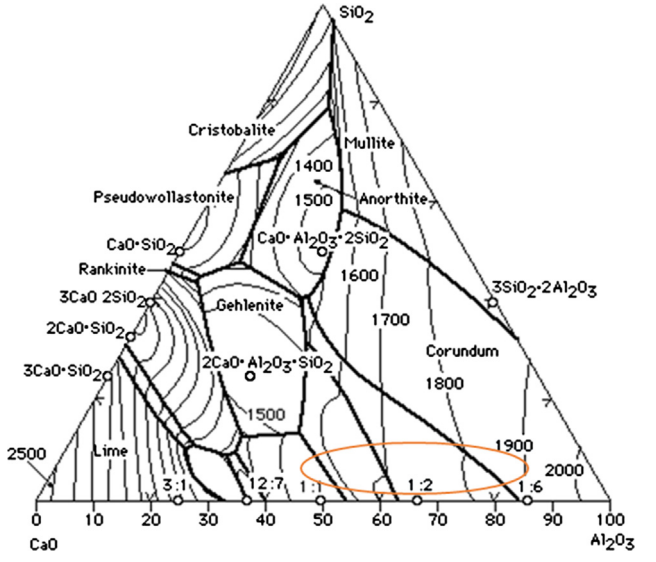

Fig. 1. Location of calcium aluminate cements in the diagram Al_2O_3-CaO-SiO_2 (TAPP 2.2; Levin et al., 1964).

Solar energy has been used in obtaining calcium aluminates (Abdurakhmanov et al., 2012). They proposed the utilization of concentrated solar energy in the synthesis of calcium aluminates with impurities of rare earth elements (Nd and Sr). The objective of Abdurakhmanov et al., 2012 was synthesizing light-generating material from calcium aluminate. First, they melted mixtures of calcium and aluminum oxides, and then after fast cooling down, the product was milled in water and Nd_2O_3 and SrO were added to the powders. The powders were compacted and sintered to obtain calcium aluminates. The research proposed by Abdurakhmanov et al., 2012, as opposed to our research, had as objective synthesizing light-generating material (absorb solar energy and reemit it in different ranges of visible light).

As we have mentioned, the production of cement is energy intensive, and is also responsible of significant CO_2 emissions. In this way, by using concentrated solar thermal (CST), CO_2 emissions could be reduced by 40% and savings could also reach the 40% as fuels and electricity are replaced with solar energy (González and Flamant, 2014; Meier et al., 2005a). Similar savings and reductions in CO_2 emissions are expected in the event of applying concentrated solar thermal to the synthesis of calcium aluminate cements. In this way, we propose the synthesis of calcium aluminates (main phases of the calcium aluminate cements) by using concentrated solar energy.

2. Experimental methodology

Experiments were carried out in a vertical axis 1.5 kW solar furnace (see Fig. 2) in the facilities of the PROMES-CNRS located in Odeillo (France). The functioning of the vertical axis solar furnace is described as follows: a solar tracking heliostat reflects the rays towards a 2.0 m in diameter parabolic concentrator (see Fig. 2), which makes converging the sun radiation at a focal point with a dimension of around 15 mm in diameter. The maximum concentration for this solar furnace is approximately 15,000 times the incident radiation. The average incident radiation took values of around 900 W/m^2 in all experiments, although during each experiment the values fluctuated in the range ± 10% of the average value for the incident radiation. The control of the power

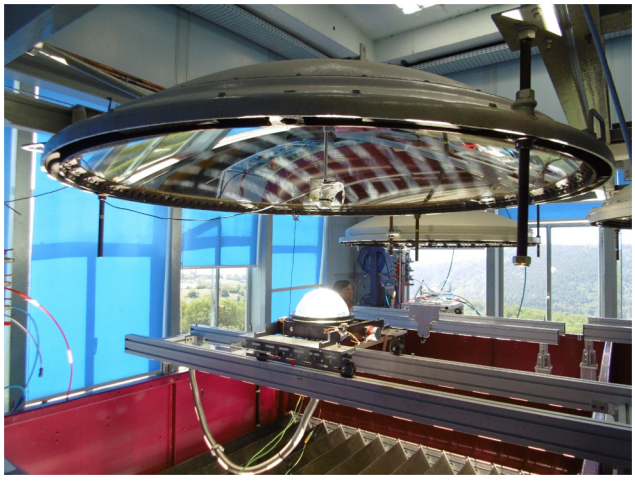

Fig. 2. 1.5 kW vertical axis solar furnace at Odeillo.

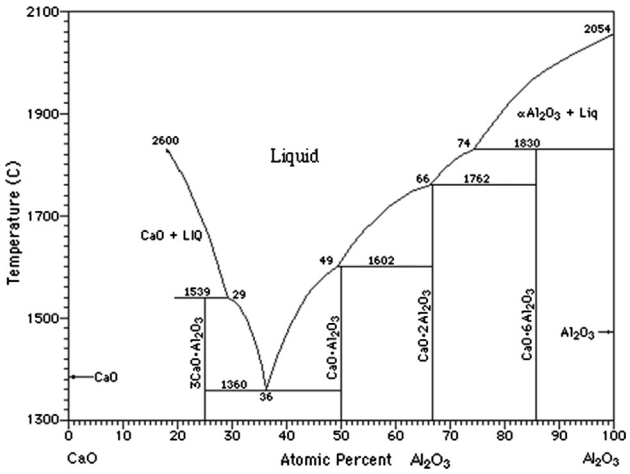

Fig. 3. CaO-Al_2O_3 binary diagram (TAPP 2.2; Levin et al., 1964).

applied in each experiment was carried out by means of a venetian blind (shutter opening, which indicates the percentage of aperture of the venetian blind, 0 closed, 100 totally opened).

The objective, as it was mentioned in the previous section, was to synthesize the typical phases that are possible to find in high alumina calcium aluminate refractory cement. This kind of cement is characterized mainly by its high alumina content (> 70% wt.), and by lime contents of around 17–30% wt., with low level of impurities (around 1%). Fig. 3 shows the CaO-Al_2O_3 phase diagram (TAPP 2.2; Levin et al., 1964) in atomic percentage. According to the amounts of alumina and lime mentioned, if the mixture is melted, during the cooling down to the room temperature, the obtained product should be mainly composed of $CaO{\cdot}2Al_2O_3$ and $CaO{\cdot}6Al_2O_3$. However, considering possible imperfections in the mixing process, which would lead to zones either enriched or impoverished in alumina, $CaO{\cdot}Al_2O_3$ and Al_2O_3 would appear in the final product.

Mixtures were prepared by using industrial quality alumina and calcium carbonate. Sodium carbonate was added as flux, while carbon was added in an attempt of increasing the emissivity of the sample because the heating of the sample is produced mainly through radiation. In this way, it is expected that the darker the mixture the higher the heat in the surface of the sample. However, it was observed that carbon was burnt at low temperatures, without effect on the emissivity. Thermocouples were placed at different points (one outside at a medium height of the crucible, see Fig. 4) and other two inside. The problem was that Cromel-Alumel thermocouples used in the experiments have 1382 °C as maximum temperature, and then they are burnt out once this temperature is surpassed. All thermocouples located

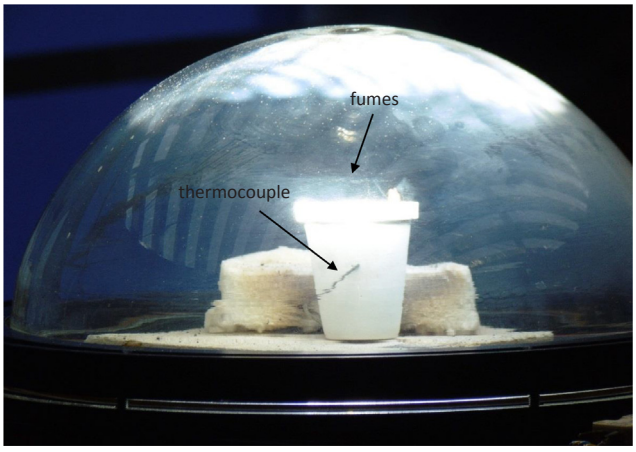

Fig. 4. Device used in the experiments.

Fig. 5. Presence of molten phase during the process.

inside were burnt during the experiment, which indicates that temperatures were significantly higher than 1400 °C. Moreover, a molten phase was observed in the crucible (see Fig. 5). All this is indicative of that temperatures were higher than that mentioned by Bensted, 2008, 1500–1600 °C, used for the synthesis of calcium aluminates in reverberatory furnaces.

Mixing was carried out manually. The initial reagents were analyzed by using x-ray fluorescence and x-ray diffraction. In the case of the carbon (Panreac) and sodium carbonate (sodium carbonate anhydrous, Probus, 99.5%) both are laboratory quality reagents. X-ray fluorescence experiments were performed with wavelength dispersive x-ray fluorescence spectrometer (Axios PANalytical) equipped with Rh-anode x-ray tube with maximum power of 4 kW. All samples were measured in vacuum with 15–50 eV energy resolution. For quantitative analysis of the spectra, the PANalytical standardless analysis package Omniam was used. X-ray diffraction measurements of powdered samples were conducted with Empyrean PANalytical diffractometer using Kα1 and Kα1 radiation from Cu anode. All measurements were performed with Bragg-Brentano setup at room temperature with the 0.006° step size at 5-90° 2θ scanning range and the 145 s of measurement time for each step. Data analysis and the peak profile fitting procedure were carried out using XPowder12 Ver. 01.02 (Database PDF2 (70 to 0.94)).

The chemical composition of the calcium carbonate is shown in Table 1, while the chemical composition of the alumina is shown in Table 2. In the case of the calcium carbonate (Table 1), we can see that carbon is not present in the results because of the measurement conditions, but the phases are identified through the x-ray diffraction analysis (Fig. 6). From the x-ray diffraction results we can check that apart from the calcium carbonate, calcium hydroxide and calcium oxide (II) are present in the initial material, although the last phase in small quantities. In Fig. 7 we see the x-ray diffraction pattern for the alumina, where we see that alumina is the main phase (different types of alumina), with peaks of aluminum trihydroxide.

Table 1
Chemical composition of the calcium carbonate.

Compound	Mass percent (%)
Na_2O	0.047
MgO	0.611
Al_2O_3	0.334
SiO_2	0.748
P_2O_5	0.017
SO_3	0.343
K_2O	0.017
CaO	97.535
MnO	0.165
Fe_2O_3	0.111
SrO	0.049
Y_2O_3	0.003
Cl	0.021

Table 2
Chemical composition of the alumina.

Compound	Mass percent (%)
Al_2O_3	98.863
SiO_2	0.533
P_2O_5	0.009
SO_3	0.151
K_2O	0.010
CaO	0.360
Fe_2O_3	0.039
Ga_2O_3	0.014
Tl_2O_3	0.001
Cl	0.021

Calcium carbonate would decompose at the temperatures of the experiments according to the following chemical reaction:

$$CaCO_3(s) \rightarrow CaO(s) + CO_2(g)$$

3029 kJ/kg CaO are required at the decomposition temperature (1173 K). In modern kiln furnaces this value ranges among 3600 kJ/kg CaO for vertical double shaft kilns and 7500 kJ/kg CaO for non-preheated long rotary kilns. The decomposition of calcium carbonate into CaO and CO_2 has been widely studied by Flamant et al., 1980, Imhof, 1997, Meier et al., 2004 and Meier et al., 2006. Similar experiments were conducted by Salman, 1988 as he studied the thermal decomposition of limestone and gypsum and obtained maximum conversions of 65% and 38%, respectively. In the case of the aluminum trihydroxide, reaction of calcination would take place at temperatures within 900 °C and 1200 °C (Sancho et al., 2000), according to the reaction:

$$2Al(OH)_3(s) \rightarrow Al_2O_3(s) + 3H_2O(g)$$

The reagents were mixed in the following proportions: 74.5% Al_2O_3, 24.5% $CaCO_3$ and 1% Na_2O (1.7% Na_2CO_3, Na_2O was used as flux, Na_2CO_3 will decompose into Na_2O and CO_2 during the heating process). Once mixed, 7.5% of carbon was added, becoming the mixture dark grey. The problem observed, as it was indicated, was that carbon is burnt at the temperatures involved in the process. It is also necessary to consider that once the thermal equilibrium is reached, the sample would not be heated up to a higher temperature, on the contrary, the sample will emit heat by radiation while heat is absorbed by the same process, remaining the temperature stable. This question is observed as a layer of treated material of approximately 20 mm in height is obtained, and below this layer the initial mixture remains unaltered.

From the analysis we see that certain impurities will leave the sample with the fumes, for instance, SO_2, Cl_2, P_2O_5, etc. Considering the proportions above mentioned, SiO_2 will be the most important impurity in the product (> 0.5%), with MgO (< 0.2%) and Na_2O (1%). In this way, silica in high quantities could lead to the formation of non-hydrating gehlenite ($2CaO{\cdot}Al_2O_3{\cdot}SiO_2$). The presence of ferrites could lead to the formation of slow setting $4CaO{\cdot}Al_2O_3{\cdot}Fe_2O_3$ or non-setting $2CaO{\cdot}Fe_2O_3$. TiO_2 could form non-setting calcium titanates.

Mixtures were loaded into tabular alumina crucibles with the following dimensions: 55 mm in height, 30 mm in upper diameter, 25 mm in lower diameter and 3 mm in thickness of the crucible walls. The crucible was located below the focal point (around 15 mm in diameter) and covered with a glass hood connected with a vacuum pump to avoid the deposition of particles in the parabolic concentrator (see Figs. 2 and 4). The presence of high temperature energy source was expected to reach the bottom of the crucible. However, and as observed when removing the sample from the crucible, the sufficient temperature was only reached in a depth of approximately 2 cm, below that point the material remained unreacted.

3. Results

Five experiments were carried out with the same mixture. As forecasted, carbon was burnt during the heating as fumes were released in all experiments (the decomposition of calcium carbonate also generated fumes), as well as because the final product was completely white at the end of the experiments. Apart from the measurements of the thermocouples, visual observation allowed to see a molten phase during the experiments (see Fig. 5).

The parameters for each experiment are shown in Table 3. The power in each sample was controlled through the shutter opening, considering the average incident radiation in each experiment. Differences with respect to the average incident radiation value were not higher than ± 10% in all experiments. The parameter time was controlled as we mentioned using a thermocouple located 2 cm below the surface of treatment as showed in Fig. 4.

Samples were analyzed by means of x-ray diffraction in powder. X-ray diffraction measurement conditions are indicated in previous sections. Results are show in Figs. 8–12.

Results from the x-ray diffraction are consistent with information collected in Fig. 3. As expected, treated samples mainly comprise $CaO2Al_2O_3$ and $CaO6Al_2O_3$. The presence of $CaO{\cdot}Al_2O_3$ and Al_2O_3 are related with the presence of areas both impoverished and enriched in alumina, respectively. In Table 4, we can see the quantitative analysis of the crystalline components (discounting amorphous phases) in mass percent. Unchecked peaks belong to impurities. The presence of unreacted starting materials (Al_2O_3, $CaCO_3$ and CaO) is expected in the sample as the material located approximately 20 mm below the surface remained unreacted. The presence of > 0.5% SiO_2 could lead to the presence of gehlenite ($2CaO{\cdot}Al_2O_3{\cdot}SiO_2$), while the presence of ferrites would lead to the formation of $4CaO{\cdot}Al_2O_3{\cdot}Fe_2O_3$ or $2CaO{\cdot}Fe_2O_3$. However, main peaks in x-ray diffraction patterns belong to calcium aluminate cements, the presence of these impurities is expected from the chemical initial analysis and would cover the points unmarked in the x-ray diffraction patterns.

Except for the sample CA2, $CaO{\cdot}2Al_2O_3$ is the main phase in all samples, as expected. The presence of $CaO{\cdot}6Al_2O_3$ is in consonance with the amount of alumina added in the process and with the binary phase diagram showed in Fig. 3. The Al_2O_3 detected could come from either a high temperature process or unreacted material. On its behalf, $CaO{\cdot}Al_2O_3$ could come from zones impoverished in Al_2O_3. According to

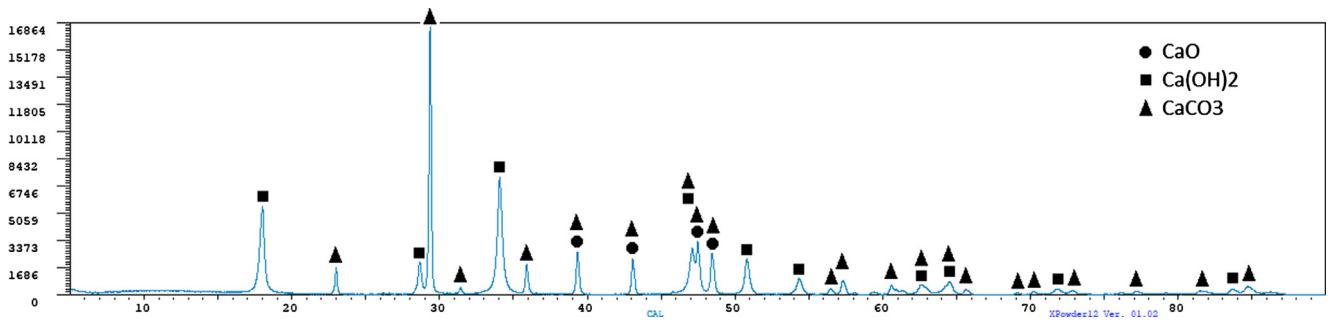

Fig. 6. X-ray diffraction pattern for the calcium carbonate.

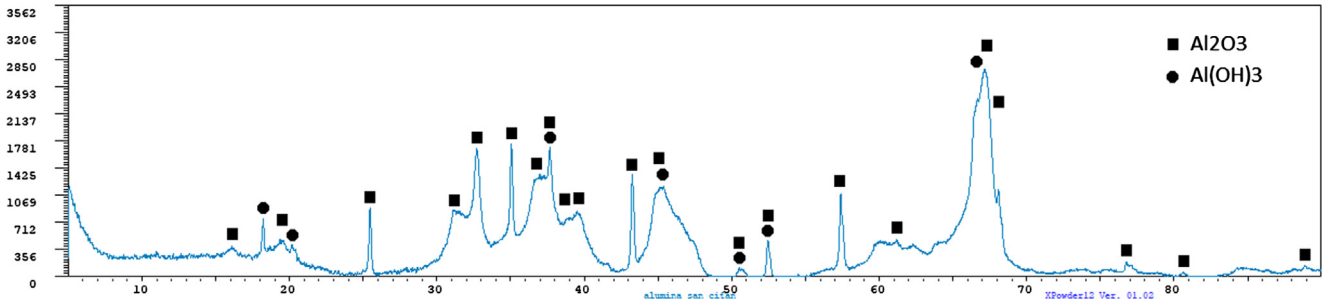

Fig. 7. X-ray diffraction pattern for the alumina.

Table 3
Conditions under what the experiments were carried out.

Sample	Shutter opening	Average incident radiation (W/m^2)	Power (kJ/s)	Time (min)
CA1	70	916	0.962	18
CA2	60	901	0.811	15
CA4	100	885	1.328	30
CA5	100	856	1.284	30
CA6	60	914	0.823	22

the results, the presence of calcium aluminate compounds (typical from high alumina refractory cements) is demonstrated, and concentrated solar energy could be considered in the manufacture of this kind of refractory cements. The quality of the calcium cement would depend on the quality of the starting materials. In this case, calcium carbonate and alumina with significant amounts of aluminum trihydroxide are used as starting reagents, so the decomposition of these phases should take place before the reaction among the constituents to form the calcium aluminates. The utilization of a renewable source of energy is expected to reduce the environmental impact as either fossil fuels or electricity are not used in the generation of heat. The costs of producing calcium aluminate via concentrated solar energy are expected to be reduced if the costs of producing this material are simplified only to the energy costs, although this question will be discussed in the next section.

A commercial calcium aluminate was analyzed by using x-ray diffraction technique (Fig. 13) to compare with the calcium aluminate obtained via concentrated solar energy.

From the analysis, it was checked that commercial calcium aluminate cements are more impure than that that we obtained in the solar furnace. As we see an important background (noise) in the x-ray diffraction analysis is indicative of that the crystallization was not complete. Identified phases are: mayenite ($Ca_{12}Al_{14}O_{33}$), grossite ($CaAl_4O_7$), alumina (Al_2O_3) and calcium aluminum oxide ($CaAl_2O_4$). This question is reasonable because temperatures involved in the industrial process (Bensted, 2008, 1500–1600 °C) seem not sufficient for the complete melting of the lime and alumina, and for the full crystallization of the calcium aluminates (see Fig. 3). In the solar process a molten phase is obtained, and thus more crystallized phases are synthsized. Calcium aluminates are clearly observed in the x-ray diffraction diagram in samples synthesized in the solar furnace, in general with a single type of calcium aluminate and with low quantities of alumina.

4. Discussion

Calcium aluminates have two main applications, as binders and as mineral reagents. As binders, the properties required for calcium aluminates are resistance to corrosion, abrasion and heat combined with rapid hardening. As reagent, calcium aluminates are used in trapping molten metal impurities in metallurgical treatments (iron and steel industry, foundry).

Solar energy has been used in obtaining calcium aluminates (Abdurakhmanov et al., 2012) to be used as light generating material. Our process follows a different line from that proposed by Abdurakhmanov et al., 2012. The objective in our case was studying the synthesis of calcium aluminates to be used as binders or reagents in the metallurgical industry, while Abdurakhmanov et al., 2012 proposed the synthesis of light-generating material from calcium aluminate. In this section, we will discuss the advantages and disadvantages of the possible industrial process to be used in the production of calcium aluminate cements.

The first step in the production of calcium aluminates via concentrated solar energy is ensuring a suitable supply of high quality raw materials. These raw materials should provide a final product with low level of impurities, for instance, high alumina cements (the group to where calcium aluminate cements belong) should present maximum amounts of Na_2O, SiO_2, Fe_2O_3 and MgO of 0.3, 0.3, 0.2 and 0.4%, respectively. These requirements are met by using high quality materials. In the case of the alumina, this product is available in the market with low level of impurities. In the experiments described in this paper, commercial alumina with the quality to be used in the Halt-Hérault process to produce aluminum was used. Metallurgical aluminas are characterized by their low level of impurities, typical values in the chemical analysis are according to Sancho et al., 2000: 50–100 ppm Si, 100–200 ppm Fe, 3500–4000 ppm Na, 200–300 ppm Ca, 50–100 ppm Ga, 5–80 ppm Zn, 15–20 ppm Ti, 5–10 ppm V, 5–10 ppm P

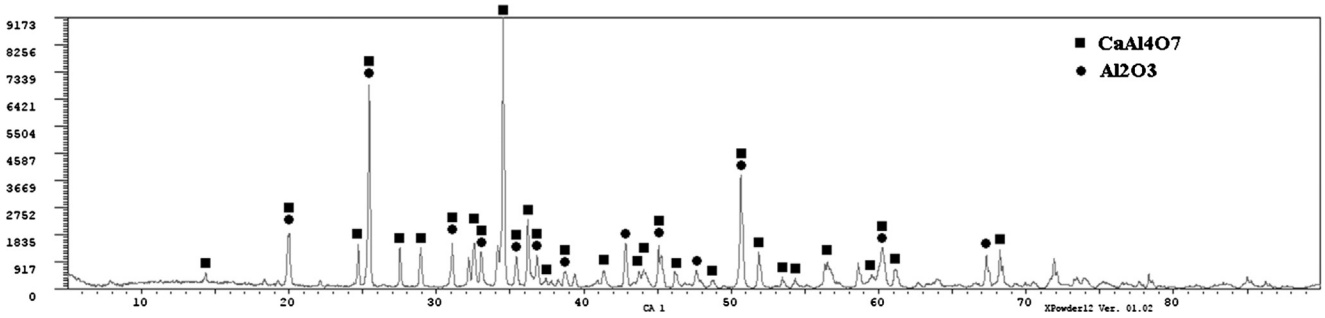

Fig. 8. X-ray diffraction pattern of the sample CA1.

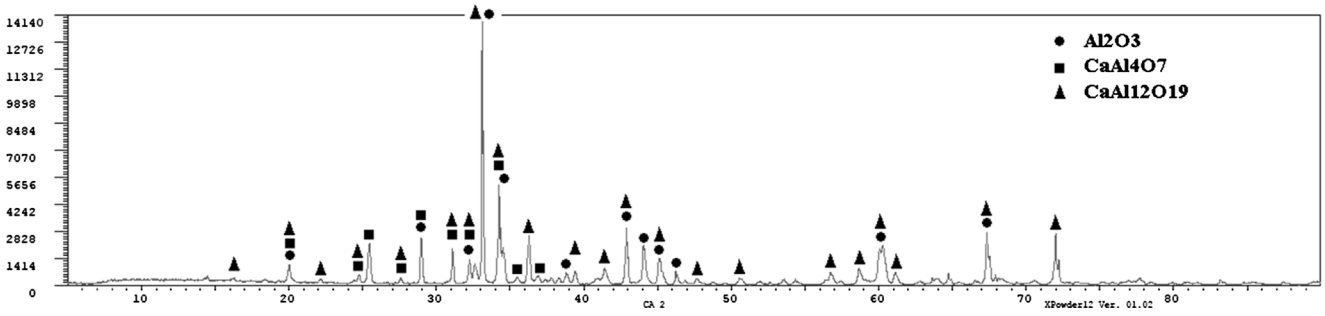

Fig. 9. X-ray diffraction pattern of the sample CA2.

and 1–5 ppm Mn. In the case of the lime, Meier et al., 2005a suggested a process to produce high purity lime via solar to be used in the chemical and pharmaceutical industries. Meier et al., 2004, Meier et al., 2005b and Meier et al., 2006 designed a kiln furnace heated indirectly by means of a system of rotatory tubes. Meier et al., 2006 used a 15 kW solar furnace. 1.5–2 h were required until stationary conditions were reached, after that the treatment lasted 30 min (1200–1400 K), with rotation speeds between 8 and 18 rpm, being the feeding rate of 36–136 g/min and particle size between 2 and 3 mm. Meier et al., 2006 observed a calcination rate of 98.2% and CaO productivity of 64.2 g/min when the temperature was 1395 K. They observed a reduction of CO_2 emissions by 20% in a state-of-the-art lime plant and up to 40% in a conventional cement plant. Meier et al., 2005a observed that for a solar calcination plant the cost of solar produced lime ranged in 2004 between: 128 and 157 $/ton for 25 MW_{th} solar plant; 137 and 170 $/ton for 5 MW_{th} solar plant; and, 169 and 198 $/ton for 1 MW_{th} solar plant. These values are approximately twice the selling price of conventional lime in 2004 (60 $/ton). Lime could be supplied as CaO, using for instance the process proposed by Meier et al., or as calcium carbonate directly as we did in our case. Using calcium carbonate instead of calcium oxide (II) avoids one step, and thus the costs of installation associated to the production of lime.

Regarding the type of solar installation, it is necessary to consider that there are limitations with respect to the temperatures that are possible to attain with one or other technologies. Cylindrical solar concentrators could be useful with the objective of operating in continuous. Heat would be supplied in a tube located at the focal line being fed the material on one side and collected on the opposite side (Fig. 14). However, this technology is limited by the temperatures that are possible to reach. According to Alarcón-Villamil et al. (2013) maximum temperatures reached by using the cylindrical solar concentrator are limited to 400 °C, and according to Jesko, 2008 to the range 150–500 °C. It would be necessary to use parabolic concentrators as higher concentrations and thus higher powers can be reached (similar to that showed in Fig. 2, but with a design that could allow treating bigger quantities than in our experiments), and they can track the sun with the heliostats. In the case of parabolic concentrators, the solar furnace could operate as a conventional submerged arc electric furnace, playing the concentrated solar beam a role similar to that of the electrode in the electric furnace (point heating), but with heating rates significantly higher.

By using the HSC 5.1 energetic requirements were calculated considering different situations:

- Using calcium oxide (II) as starting material or using calcium carbonate as starting material.
- Producing $CaO{\cdot}2Al_2O_3$ (2AC) or producing $CaO{\cdot}\ Al_2O_3$ (AC).

Results are displayed in Table 5.

In situations A and B, supplying calcium oxide (II) is necessary (CO_2 emissions and energy consumptions would be associated to this additional process). In situations C and D, calcium carbonate is used, and CO_2 associated to the decomposition of the calcium carbonate would be released to the atmosphere, and energy requirements would be higher because of the energy requirements for the limestone decomposition reaction.

Now we will consider two situations: a plant producing 1000 tons of calcium aluminates (CA) yearly and a plant producing 10,000 tons of calcium aluminate yearly. We will use information provided by Flamant et al. (1999) and Meier et al. (2005a) to estimate the energy requirements in the case of using concentrated solar energy. We assume a plant operating 2677 h/year as Meier et al. (2005a). According to Flamant et al. (1999), for a solar furnace the overall efficiency (optical) reaches the 60%. We assume an efficiency in the process of the 45% (the same as in Meier et al. (2005a) for the kiln furnace). Under these conditions, the power input required would be in the case of a 1000 t CA/year and 10,000 t CA/year that showed in Tables 6 and 7.

The production of calcium aluminates is not excessively important in quantities worldwide, so plants for 1000 t CA/year or 10,000 t CA/year could be sufficient to supply enough product for the market.

Now, we are going to compare the CO_2 emissions of the solar process and the electric process (electric furnace). According to the IEA (International Energy Agency) carbon dioxide emissions for electricity in Europe are 0.4537 kg CO_2/kWh. In the case of the electric furnace we assume an efficiency of 60% to calculate the theoretical energy requirements. Considering the situations described in Table 5, the energy

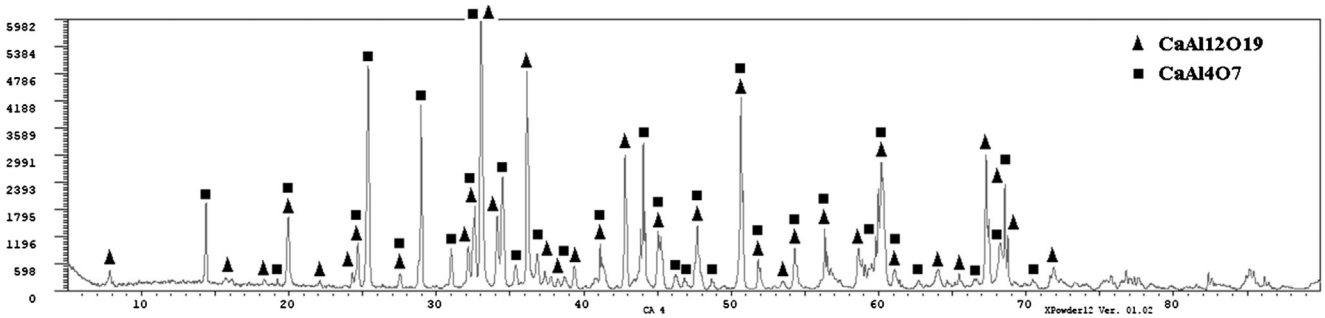

Fig. 10. X-ray diffraction pattern of the sample CA4.

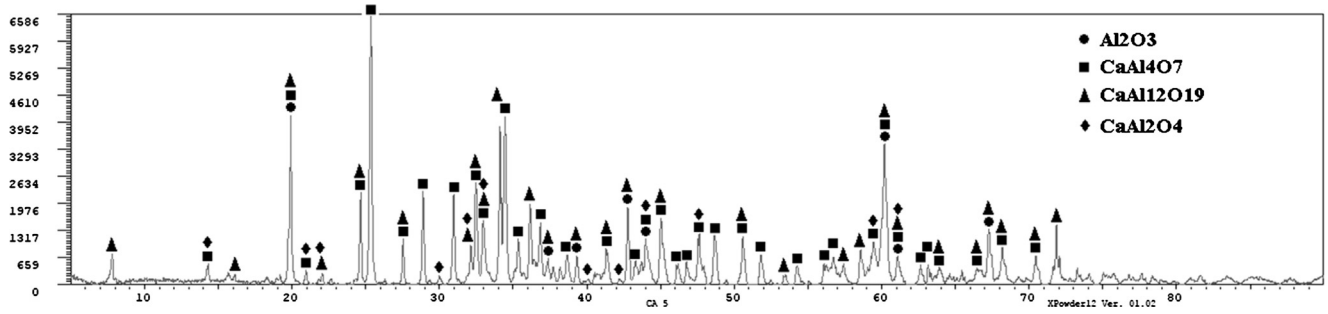

Fig. 11. X-ray diffraction pattern of the sample CA5.

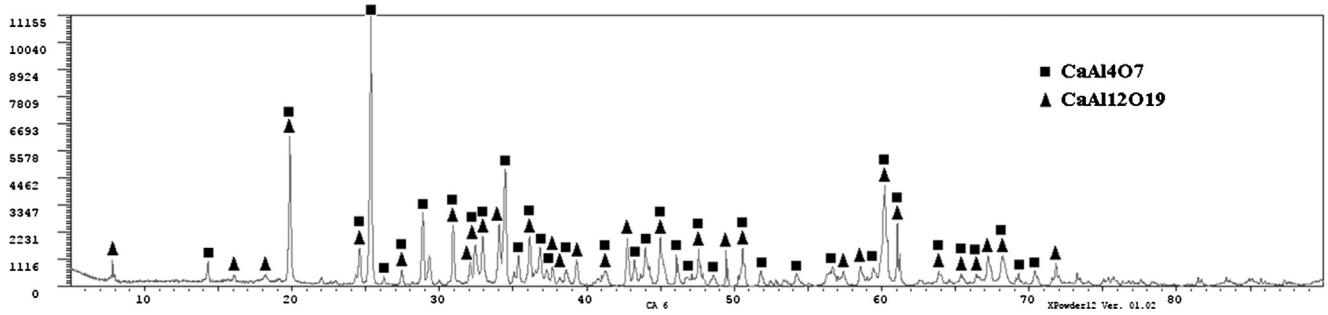

Fig. 12. X-ray diffraction pattern of the sample CA6.

Table 4
Quantitative analysis of the crystalline components (mass percent).

	CA1	CA2	CA4	CA5	CA6
$CaO{\cdot}2Al_2O_3$	90.5 ± 0.7	15.8 ± 0.7	62.7 ± 0.9	59.6 ± 1.0	85.3 ± 0.8
Al_2O_3	9.6 ± 1.2	27.4 ± 0.4		11.9 ± 2.0	
$CaO{\cdot}6Al_2O_3$		56.8 ± 0.4	37.4 ± 1.6	24.3 ± 1.8	14.7 ± 1.6
$CaO{\cdot}Al_2O_3$				4.2 ± 2.1	

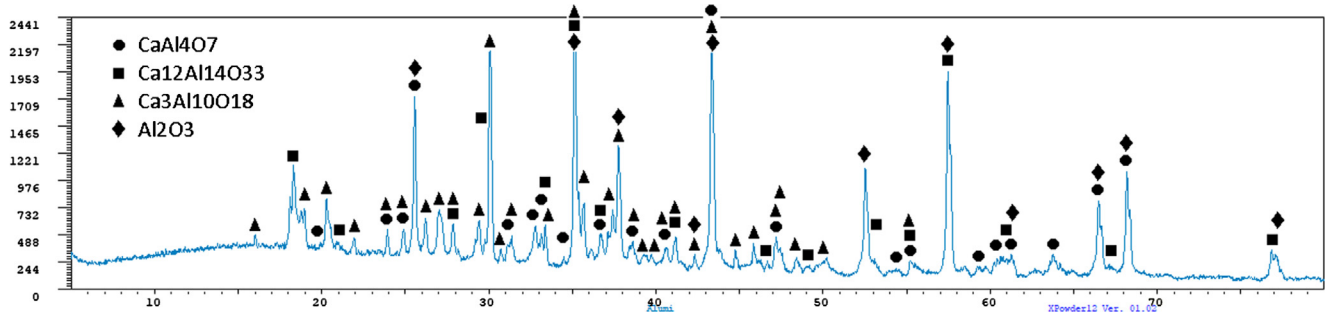

Fig. 13. X-ray diffraction diagram for a commercial calcium aluminate.

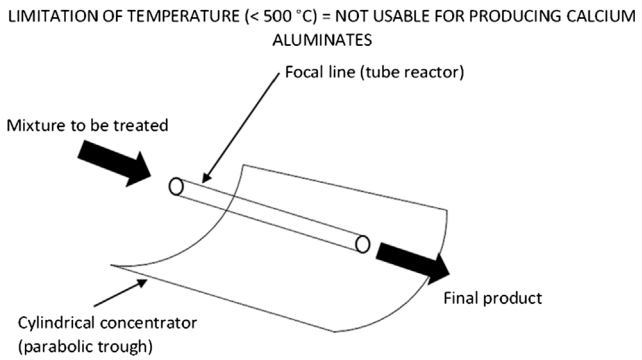

Fig. 14. Scheme of the parabolic concentrator.

Table 5
Energy required to produce 1 t of calcium aluminate. Conditions $T_{initial}$ = 25 °C and T_{final} = 1600 °C.

Situation A	$CaO + Al_2O_3$	$CaO{\cdot}2Al_2O_3$	472 $kWh{\cdot}t^{-1}$ 2AC
Situation B	$CaO + Al_2O_3$	$CaO{\cdot}Al_2O_3$	447 $kWh{\cdot}t^{-1}$ AC
Situation C	$CaCO_3 + Al_2O_3$	$CaO{\cdot}2Al_2O_3$	751 $kWh{\cdot}t^{-1}$ 2AC
Situation D	$CaCO_3 + Al_2O_3$	$CaO{\cdot}Al_2O_3$	907 $kWh{\cdot}t^{-1}$ AC

requirements for the solar process presented in Table 6 and the energy requirements in the electric furnace (efficiency of 60%), the CO_2 emissions for both the electric furnace and the solar via are collected in Table 8.

In this way, CO_2 emissions would be significantly reduced in the event of using concentrated solar energy if compared with the electric furnace. In situations C and D, CO_2 emissions belong to the calcination

Table 6
Power requirements for a plant producing 1000 t CA/year.

	Initial (theoretical)	Energy (1000 t CA/year) Optical + Process	Power (1000 t CA/year) Optical + Process
Situation A	472 kWh·t^{-1} 2AC	1748 kWh·t^{-1} 2AC	653 kW
Situation B	447 kWh·t^{-1} AC	1656 kWh·t^{-1} AC	619 kW
Situation C	751 kWh·t^{-1} 2AC	2781 kWh·t^{-1} 2AC	1039 kW
Situation D	907 kWh·t^{-1} AC	3359 kWh·t^{-1} AC	1255 kW

Table 7
Power requirements for a plant producing 10,000 t CA/year.

	Initial (theoretical)	Energy (10,000 t CA/year) Optical + Process	Power (10,000 t CA/year) Optical + Process
Situation A	472 kWh·t^{-1} 2AC	1748 kWh·t^{-1} 2AC	6530 kW
Situation B	447 kWh·t^{-1} AC	1656 kWh·t^{-1} AC	6190 kW
Situation C	751 kWh·t^{-1} 2AC	2781 kWh·t^{-1} 2AC	10,390 kW
Situation D	907 kWh·t^{-1} AC	3359 kWh·t^{-1} AC	12,550 kW

Table 8
CO_2 estimated emissions for both the electric and solar processes.

	Energy solar	Energy electric furnace	kg CO_2/t AC or t 2AC	
	Optical + Process		Electricity	Solar
Situation A	1748 kWh·t^{-1} 2AC	786 kWh·t^{-1} 2AC	356.6	–
Situation B	1656 kWh·t^{-1} AC	745 kWh·t^{-1} AC	338	–
Situation C	2781 kWh·t^{-1} 2AC	1251 kWh·t^{-1} 2AC	767	169
Situation D	3359 kWh·t^{-1} AC	1512 kWh·t^{-1} AC	964	278

of the calcium carbonate.

Some other considerations should be taken into account in the design of the process. Due to the specific characteristics of the heat transfer in a solar furnace, sun radiation energy is found in a small surface section where it is possible to reach 1040–1650 $W \cdot cm^{-2}$. This question propitiates a heat energy transfer in cents of second to a charge that presents a thermal diffusivity of $L^2 \cdot T^{-1}$:

$$\alpha(L^2 \cdot T^{-1}) = \frac{\lambda}{c_p \cdot \rho}$$

where λ is the thermal conductivity, c_p is the specific heat, and ρ the density of the materials affected by the radiation. This parameter, thermal diffusivity, can be an instrument of interest for the design of a solar furnace, where the load could reach the molten state in a few seconds and then displacing the load at speed, v, as a function of the thickness, t, affected by the radiation that causes the melting:

$$\alpha = v \cdot t$$

This question is related with the formation of a crust of reacted material in a depth of approximately 20 mm in height, while below this layer the material remains unreacted. The presence of unreacted material is related with the capacity of the heat to reach the lower zones of the crucible through diffusion mechanisms. It is expected that with a higher power the heat would reach a higher depth, and the volume of material treated would be significantly larger. If the heat does not reach the whole volume of material in our experiments during the time while they were held under the concentrated solar beam, it is assumed that once the thermal equilibrium was reached and reactions took place, the remaining time calcium aluminates were kept at high temperature and the rest of the heat is re-emitted through the radiation heat transfer mechanism. According to the volume of material treated, the time required to heat the initial materials up to the reaction temperature is shorter and the process could take not more than 15 min. In this way, the temperature for the process should be controlled with other kind of mechanisms that could indicate the temperature of the molten phase and once the reaction temperature was reached, the process could be finished. In this moment, new non-treated material could be displaced to a point below the focal point through a continuous system of buckets, or discontinuously by treating the material in a crucible and then pouring it and loading new material in the crucible.

Even when the initial investment to produce the calcium aluminates would be important, it is expected that once installed, production costs would be significantly lower in the case of the concentrated solar energy if compared with the production through the conventional process (considering only the cost of providing energy for the process, according to González and Flamant (2014), using concentrated solar thermal could reduce a 40% the costs in the cement industries). However, several questions arise when exploring (apart from that mentioned throughout the paper) the production of calcium aluminates via concentrated solar energy: the location of sun better conditions usually far from the main consumption centers (transportation costs) or the appearance of new taxes to renewable energies.

5. Conclusions

In the present work, the feasibility of obtaining calcium aluminates by using concentrated solar energy was investigated. The pursued calcium aluminate cement compounds were obtained. The basic concluding remarks can be summarized as follows:

- $CaO{\cdot}2Al_2O_3$ is obtained as expected, being the main phase in calcium aluminate refractory cements together with $CaO{\cdot}6Al_2O_3$.
- The obtaining of $CaO{\cdot}2Al_2O_3$ and $CaO{\cdot}6Al_2O_3$ through concentrated solar energy power offers a new field of application of solar energy. The advantages regarding the conventional methods for obtaining this refractory cement are: the avoiding of contaminants added to the product through conventional fossil fuels; the environmental improvements (CO_2 emissions would be reduced); and the economic questions. Moreover, it is possible to say that refractory calcium aluminate cement is a high added value product that can makes interesting concentrated solar energy as power source for its obtaining.

Acknowledgements

Financial support by the Access to Research Infrastructures activity in the 7th Framework Program of the EU (SFERA 2 Grant Agreement n. 312643) is gratefully acknowledged and the use of the facilities and its researchers/technology experts.

This research was supported by the Ministerio de Educación, Cultura y Deportes of Spain via an FPU (Formación del Profesorado Universitario) grant to one of the authors: Daniel Fernández González (grant number FPU014/02436).

References

Abdurakhmanov, A.A., Paizullakhanov, M.S., Akhadov, Zh., 2012. Synthesis of calcium aluminates on the big solar furnace. Appl. Solar Energy 48 (2), 129–131.
Alarcón-Villamil, A., Hortúa, J.E., López, A., 2013. Comparizon of thermal solar collector technologies and their applications. Tecciencia 8 (15), 129–131.
Bensted, J., 2008. Calcium aluminate cements, 2nd ed. Spon Press (Taylor and Francis Group), London, pp. 114–139.
Cardarelli, F., 2008. Material Handbook. A Concise Desktop Reference, 2nd ed. Springer-Verlag, London Limited, London.
Ceballos-Mendivil, L.G., Cabanillas-López, R.E., Tánori-Córdova, J.C., Murrieta-Yesca, R., Pérez-Rábago, C.A., Villafrán-Vidales, H.I., Arancibia-Bulnes, C.A., Estrada, C.A., 2015. Synthesis of silicon carbide using concentrated solar energy. Sol. Energy 116, 238–246.

Costa-Oliveira, F.A., Guerra-Rosa, L., Cruz-Fernandes, J., Rodríguez, J., Cañadas, I., Martínez, D., Shohoji, N., 2009. Mechanical properties of dense cordierite discs sintered by solar radiation heating. Mater. Trans. 50 (9), 2221–2228.
Cruz-Fernandes, J., Guerra, L., Martínez, D., Rodríguez, J., Shohoji, N., 1998. Influence of gas environment on synthesis of silicon carbide through reaction between silicon and amorphous carbon in a solar furnace at PSA (Plataforma Solar de Almería). J. Ceram. Soc. Jpn. 106 (1236), 839–841.
Cruz-Fernandes, J., Amaral, P.M., Guerra-Rosa, L., Martínez, D., Rodríguez, J., Shohoji, N., 1999. X-ray diffraction characterization of carbide and carbonitride of Ti and Zr prepared through reaction between metal powders and carbon powders (graphitic or amorphous) in a solar furnace. Int. J. Refract. Metal. Hard Mater. 17 (6), 437–443.
Cruz-Fernandes, J., Amaral, P.M., Guerra-Rosa, L., Shohoji, N., 2000. Weibull statistical analysis of flexure breaking performance for alumina ceramic disks sintered by solar radiation heating. Ceram. Int. 26 (2), 203–206.
Cruz-Fernandes, J., Anjinho, C., Amaral, P.M., Guerra-Rosa, L., Rodríguez, J., Martínez, D., Almeida Costa Oliveira, F., Shohoji, N., 2002. Characterization of solar-synthesised TiC_x (x = 0.5, 0.625, 0.75, 0.85, 0.90 and 1.0) by x-ray diffration, density and Vickers microhardness. Mater. Chem. Phys. 77 (3), 711–718.
Fernández-González, D., Ruiz-Bustinza, I., González-Gasca, C., Piñuela-Noval, J., Mochón-Castaños, J., Sancho-Gorostiaga, J., Verdeja, L.F., 2018. Concentrated solar energy applications in materials science and metallurgy. Sol. Energy 170, 520–540.
Flamant, G., Hernandez, D., Traverse, J., 1980. Experimental aspects of the thermochemical conversion of solar energy; Decarbonation of CaCO3. Sol. Energy 24 (4), 385–395.
Flamant, G., Ferriere, A., Laplaze, D., Monty, D., 1999. Solar processing of materials: opportunities and new frontiers. Sol. Energy 66 (2), 117–132.
Flamant, G., Balat-Pichelin, M., 2010. Elaboration and testing of materials using concentrated solar energy. Encyclopedia of Life Support Systems. Eolss Publishers Co. Ltd./UNESCO, United Kingdom, pp. 363–389.
García-Cambronero, L. E., Cañadas, I., Díaz, J. J., Ruíz-Román, J. M. and Martínez, D., 2008, Tratamiento térmico de espumación de precursores de aluminio-silicio en horno solar de lecho fluidificado. In: Proceedings of the X Congreso Nacional de Materiales, San Sebastián, Spain, pp. 261–264.
García-Cambronero, L.E., Cañadas, I., Martínez, D., Ruíz-Román, J.M., 2010. Foaming of aluminium-silicon alloy using concentrated solar energy. Sol. Energy 84, 879–887.
González, R.S., Flamant, G., 2014. Technical and economic feasibility analysis of using concentrated solar thermal technology in the cement production process: hybrid approach – a case study. J. Sol. Energy Eng. 136 (2), 025001–025012.
Gosh, G.K., 1991. Solar Energy, The Infinite Source. APH Publishing Corporation, New Dehli.
Guerra-Rosa, L., Miguel-Amaral, P., Anjinho, C., Cruz-Fernandes, C., Shohoji, N., 2002. Fracture toughness of solar-sintered WC with Co additive. Ceram. Int. 28 (3), 345–348.
Gulamova, D.D., Uskenbaev, D.E., Turdiev, Zh.Sh., Toshmurodov, Yo.K., Bobokulov, S.H., 2009. Synthesis of silicon carbide by exposure to solar radiation. Appl. Solar Energy 45 (2), 105–108.
Herranz, G., Romero, A., de Castro, V., Rodríguez, G.P., 2013. Development of high speed steel sintered using concentrated solar energy. J. Mater. Process. Technol. 213, 2065–2073.
Herranz, G., Romero, A., de Castro, V., Rodríguez, G.P., 2014. Processing of AISI M2 high speed steel reinforced with vanadium carbide by solar sintering. Mater. Des. 54, 934–946.
Imhof, A., 1997. Decomposition of limestone in a solar reactor. Renewable Energy 10 (2/3), 239–246.
Jesko, Z., 2008, Classification of solar collectors. In: Proceedings of the 7th International Scientific Conference in Engineering for Rural Development, Jelgava, Latvia, pp. 22–27.
Kurdowski, W., 2014. Cement and Concrete Chemistry. Springer, Dordrecht.
Levin, E.M., Robbins, C.R., McMurdie, H.F., 1964. Phase Diagrams for Ceramists. The American Ceramic Society, Columbus, Ohio.
Llorente, J., Vázquez, A.J., 2009. Solar hardening of steel with a new scale solar concentrator. Mater. Chem. Phys. 118, 86–92.
McDonald, D., Hunt, L.B., 1982. A History of Platinum and Allied Metals. Ed. Johnson Matthey, Hatton Garden, London.
Meier, A., Bonaldi, E., Cella, G.M., Lipinski, W., Wuillemin, D., Palumbo, R., 2004. Design and experimental investigation of a horizontal rotary reactor for the solar thermal production of lime. Energy 29, 811–821.
Meier, A., Gremaud, N., Steinfeld, A., 2005a. Economic evaluation of the industrial solar production of lime. Energy Convers. Manage. 46, 905–926.
Meier, A., Bonaldi, E., Cella, G.M., Lipinski, W., 2005b. Multitube rotary kiln for the industrial solar production of lime. J. Sol. Energy Eng. 127 (3), 386–395.
Meier, A., Bonaldi, E., Cella, G.M., Lipinski, W., Wuillemin, D., 2006. Solar chemical reactor technology for industrial production of lime. Sol. Energy 80, 1355–1362.
Mochón, J., Ruiz-Bustinza, I., Vázquez, A., Fernández, D., Ayala, J.M., Barbés, M.F., Verdeja, L.F., 2014. Transformations in the Iron-Manganese-Oxygen-Carbon system resulted from treatment of solar energy with high concentration. Steel Res. Int. 85, 1469–1476.
Murray, J.P., Flamant, G., Roos, C.J., 2006. Silicon and solar-grade silicon production by solar dissociation of Si3N4. Sol. Energy 80, 1349–1354.
Newcomb, S., 2009. The World in a Crucible: Laboratory Practice and Geological Theory at the Beginning of Geology. The Geological Society of America Inc, Boulder, Colorado.
Osinga, T., Frommherz, U., Steinfeld, A., Wieckert, C., 2004. Experimental investigation of the solar carbothermic reduction of ZnO using a two cavity solar reactor. J. Sol. Energy Eng. 126, 633–637.
Pero-Sanz, J.A., Quintana, M.J., Verdeja, L.F., 2017. Solidification and Solid-state Transformations of Metals and Alloys. Elsevier, Amsterdam.
Román, R., Cañadas, I., Rodríguez, J., Hernández, M.T., González, M., 2008. Solar sintering of alumina ceramics: microstructural development. Sol. Energy 82, 893–902.
Ruiz-Bustinza, I., Cañadas, I., Rodríguez, J., Mochón, J., Verdeja, L.F., García-Carcedo, F., Vázquez, A., 2013. Magnetite production from steel wastes with concentrated solar energy. Steel Res. Int. 84, 207–217.
Salman, O.A., 1988. Thermal decomposition of limestone and gypsum by solar energy. Sol. Energy 41 (4), 305–308.
Sancho, J.P., Verdeja, L.F., Ballester, A., 2000. Metalurgia extractiva. Procesos de Obtención. Ed. Síntesis, Madrid.
Scrivener, K., 2003. In: Newman, J., Seng Choo, B. (Eds.), Advanced Concrete Technology. Butterworth-Heinemann (Elsevier), Oxford.
TAPP. Version 2.2. ES Microware Inc., Wade Court, Hamilton, OH.
Verdeja, L.F., Sancho, J.P., Ballester, A., 2008. Materiales Refractarios y Cerámicos. Ed. Síntesis, Madrid.
Verdeja, L.F., Sancho, J.P., Ballester, A., González, R., 2014. Refractory and Ceramic Materials. Ed. Síntesis, Madrid.
Zhilinska, N., Zalite, I., Rodríguez, J., Martínez, D., Cañadas, I., 2003. Sintering of Nanodisperse Powders in a Solar Furnace, EUROPM2003. Sintering 423–428.